Infrared, Conductance, and Kinetic Evidence for Alkali Metal Ion Interactions with Derivatives of Manganese Carbonylates

M. York Darensbourg,* D. J. Darensbourg,* Drusilla Burns, and D. A. Drew[1]

Contribution from the Department of Chemistry, Tulane University, New Orleans, Louisiana 70118. *Received September 3, 1975*

Abstract: A combination of ir, kinetic, and conductivity data has been used to define the nature and importance of ion-pairing phenomena in alkali metal manganese carbonylates. Infrared analysis indicates the contact ion interactions observed for $NaMn(CO)_4L$ (L = PMe_2Ph, PPh_3, $P(OPh)_3$, and CO) to be that of Na^+ interacting with the oxygen of an equatorial CO group. Conductometric titrations indicate specific interaction of two to four HMPA molecules per Na^+ or Li^+ and one 15-crown-5-macrocyclic polyether per Na^+ or Li^+ in the formation of solvent-separated ion pairs and free ions of $M^+Mn(CO)_5^-$. The importance of these complexed cations is manifest in the activation parameters for reactions of alkyl halides with $M^+Mn(CO)_4L^-$ (L = CO and $P(OPh)_3$) in THF. In the presence of a cation-complexing agent such as HMPA, the rate of addition of RX to form *cis*-$RMn(CO)_4L$ is drastically lowered as a result of a larger negative entropy of activation. Center-to-center distance parameters and dissociation constants for ion pairs as derived from conductance dependence on concentration are discussed in terms of the electronic nature of the anion and the solvation sphere of the cation. A particularly interesting observation on distance parameters as related to asymmetric anions is noted.

The role of ion pairing in reactions of carbanions has received an enormous amount of attention from organic and physical chemists.[2-4] Similar ion-pairing effects on chemical reactivity of transition metal organic anions have not been well-defined although the physical phenomenon of group 1a and 2a metal ion interactions with the carbonyl oxygen in transition metal carbonylates is well documented. The crystal structure of $[\eta^5\text{-}C_5H_5Mo(CO)_3]_2Mg(C_5H_5N)_4$ is known to contain a planar py_4Mg^{+2} with the two remaining octahedral sites occupied by one carbonyl oxygen of two adjacent $\eta^5\text{-}C_5H_5Mo(CO)_3^-$.[5] Identification of interaction in solution has been based principally on the analysis of infrared spectra either in the ν(CO) region or in the far infrared where cation–solvent cage rattling motions may be observed. Thus $NaCo(CO)_4$ was shown by Edgell et al. to consist of an equilibrium of solvent separated and contact ion pairs, $(CO)_3CoCO^-\cdots Na^+$, in tetrahydrofuran.[6] Other more recent solution studies of interactions include compounds such as $LiMn(CO)_5$,[7] $NaMn(CO)_5$,[7] $NaRFe(CO)_4$,[8] and $Li[Ph_3PFe(CO)_3C(O)Ph]$.[9]

Infrared spectroscopy in the ν(CO) region has been a most valuable aid in distinguishing between interactions involving direct contact of anion(s) and cation(s) and less associated forms, such as solvent-separated ion pairs and free ions. However due to similar, if not identical, symmetries and immediate solvent shells of the free carbonylate anion and the anion in the solvent-separated ion pair environment, these less associated forms are expected to be spectroscopically indistinguishable. Data from chemical studies and conductivity measurements may also be used to infer the nature of possible species in solution. In this connection we wish to report observations of ion-pairing phenomena in alkali salts of $Mn(CO)_4L^-$ (L = Ph_3P, $(PhO)_3P$, and Me_2PhP) in ether solvents employing a combination of ν(CO) infrared spectral studies, conductivity measurements, and alkyl halide reaction kinetics. The reactions of alkyl halides (RX) with $Mn(CO)_5^-$ or $Mn(CO)_4L^-$ form $RMn(CO)_5$ or *cis*-$RMn(CO)_4L$ derivatives, respectively. The dependence of such reactions on counterion, substituent ligand L, alkyl halide, and solvent–solvent mixture has been extensively investigated. These studies have allowed for some distinction between the principal types of solution interactions that can occur in alkali metal salts of $Mn(CO)_4L^-$.

Experimental Section

Materials. Solvents or complexing agents were purified by distillation under N_2 from an appropriate scavenging agent immediately prior to use: tetrahydrofuran, from the purple sodium benzophenone dianion; diethyl ether, from sodium wire; hexamethylphosphoric triamide (HMPA) (Eastman), from sodium. The crown ether, 15-crown-5, purchased from Peninsular Chem-Research was not further purified; however, as checked by gas chromatography, ir, and NMR, no more than a 2–3% impurity was present. Manganese decacarbonyl was a generous gift from the research group of Professor Gerard Dobson. The organic halides were reagent grade and used without further purification.

Preparations. Reactions were run under an atmosphere of N_2; utmost precautions were used for the exclusion of air. Sodium manganesepentacarbonyl and $LiMn(CO)_5$ were prepared by adding a THF solution of $Mn_2(CO)_{10}$ of known concentration to a flamed, N_2 flushed flask containing dilute sodium amalgam or shiny lithium wire. Diethyl ether solutions of $NaMn(CO)_5$ were prepared by complete removal of THF under vacuum and redissolving in Et_2O. Substituted analogues, $NaMn(CO)_4PR_3$ (PR_3 = PPh_3, $P(OPh)_3$, and PMe_2Ph), were similarly prepared from the previously reported dimers, $[R_3PMn(CO)_4]_2$.[10] Cleavage of the dimers by Na or Li is complete. This was checked by quantitative formation of $MeMn(CO)_4L$ (L = PR_3 or CO) from solutions of the salts.

Kinetic Measurements. The kinetic studies were carried out in oven-dried 50 ml erlenmeyer flasks which were securely fitted with rubber septum caps. A measured THF or diethyl ether solution of the respective manganese carbonyl anion of known concentration was introduced into the argon flushed flasks by syringe. The reaction flasks were placed in a Tamson constant-temperature bath equipped with a Portable Bath Cooler with a constant-temperature control of ±0.05 °C. After the solutions were allowed to equilibrate to temperature, the alkyl halide was accurately added to the flask employing a syringe and the reactants were thoroughly mixed. Samples for ir spectral analysis were withdrawn periodically with a syringe and placed in a sealed 0.1 mm pathlength NaCl infrared cell. Rates of reaction were observed by following the decrease in absorption of the reactants' most intense ν(CO) vibration, the E mode. Pseudo-first-order reaction conditions using at least a ten-fold excess of alkyl halide were employed where appropriate. Reactions too fast to be followed conventionally under pseudo-first-order conditions were measured under second-order reaction conditions using equal concentrations of carbonyl anion and alkyl halide.

Rate constants were calculated using a linear-least-squares program for the first-order rate plots of $\ln (A_t - A_\infty)$ vs. time, where A_t is the absorbance at time t and A_∞ is the absorbance at time infinity. For reactions carried out under second-order conditions a least-squares

Table I. Infrared Data in the ν(CO) Region for $NaMn(CO)_5$, $LiMn(CO)_5$, and $NaMn(CO)_4PR_3$ in Various Ether Solvent Systems[a]

Salt	Solvent[b]	A_2''[c]		E′		$\nu(CO\cdots M^+)$	
$NaMn(CO)_5$	HMPA/THF	1893.7 (s)		1860.7 (s)			
	15-Crown-5/THF	1893.7 (s)		1860.0 (s)			
	THF[d]	*1901.7 (s)*	1897.0 (s)	*1875.1 (s)*	1862.3 (s)	*1828.6 (m)*	
	Et_2O[d]	*1912.2 (s)*		*1882.9 (s)*		*1803.7 (m)*	
$LiMn(CO)_5$	HMPA/THF	1893.1 (s)		1860.0 (s)			
	THF	1894.7 (s)		1861.4 (s)			

		A[e]	A_1	A	A_1	A′	E	A(CO···M⁺)
$NaMn(CO)_4P(OPh)_3$	HMPA/THF		1963.2 (m)		1868.7 (m)		1838.2 (s)	
	THF	*1964.1 (m)*	1960.0 (w)	*1875.7 (m)*		*1848.4 (s)*	1838.0 (m)	*1800.3 (s)*
$NaMn(CO)_4PPh_3$	HMPA/THF		1940.8 (m)		1845.2 (m)		1812.7 (s)	
	THF	*1943.5 (m)*	1938.7 (w)	*1852.7 (m)*		*1826.7 (s)*	1812.7 (m)	*1774.3 (s)*
$NaMn(CO)_4PMe_2Ph$	HMPA/THF		1935.6 (m)		1838.6 (m)		1803.0 (s)	
	THF	*1940.8 (m)*	1934.7 (w)	*1847.6 (m)*		*1817.1 (s)*	1802.5 (m)	*1767.7 (m)*

[a] Frequencies in italics are assigned to the contact ion species. [b] Approximately 10 equiv of HMPA per Li^+ or Na^+ ion; 1 equiv of 15-crown-5 per Na^+ ion. [c] The two infrared active vibrations for a solvent-separated or free ion pair of D_{3h} symmetry are of A_2'' and E symmetry. [d] Positive assignment of weak bands previously reported[7] near 2020 cm^{-1} is impossible due to trace $Mn_2(CO)_{10}$ contaminant. [e] 3A + A′ are the symmetry labels for the contact ion involving Na^+ interaction with an equatorial CO ligand, whereas the symmetry labels for a solvent separated or free ion (C_{3v}) species are $2A_1$ + E.

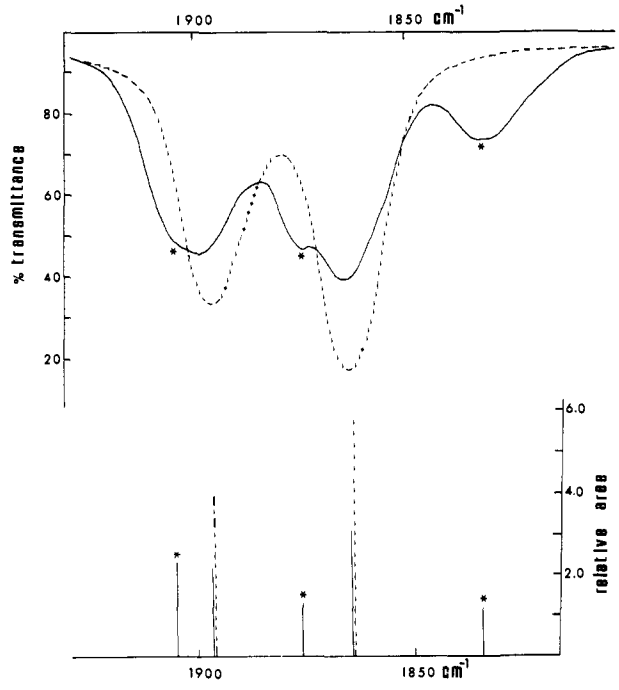

Figure 1. ν(CO) spectra of $NaMn(CO)_5$ (* absorptions due to contact ion species): (—) 0.0067 M in THF; (- - -) 0.0067 M in THF with 20 equiv of HMPA to Na^+ added. The relative band areas were obtained via band shape analysis. The intensity ratio for the two high-frequency absorptions in the contact ion species in THF is 1.7 and in Et_2O this ratio is 1.4.

program for plots of $1/(A_t - A_\infty)$ vs. time was employed. Absorbance values were converted to concentration units by multiplying the slope of such a plot by ϵb where b is the pathlength of the cell and ϵ is the extinction coefficient for the band being observed.

Products were identified by their infrared spectra as compared with previously isolated compounds characterized in our laboratories.[11]

Conductivity Measurements. Resistivities of solutions were measured on a Serfass Conductivity Bridge, Model RCM15B1, or a Barnstead Conductivity Bridge, Model PM 70CB (range of 0.1 to 10^7 ohms, with a reported maximum error of ±1 to ±3% within this range). The conductivity cell used was a Beckman Instruments Company Model CEL-3A with a 15 ml chamber volume. Shiny platinum electrodes are fixed rigid in the cell whose constant was determined to be 0.238 cm^{-1} (0.100 demal KCl solution according to Jones and Bradshaw).[12] In a typical concentration study the cleaned and dried cell, fitted with a wired-on rubber septum, was flushed with nitrogen, rinsed with quantities of the freshly prepared carbonylate solution until constant resistance readings were achieved, and rinsed further with the pure THF. An exact quantity of THF was then syringed into the empty cell chamber, and successive aliquots of the carbonylate solution added via microliter syringe. Mixing was achieved by gently swirling the cell. All studies were carried out at 26.0 °C.

Spectral Measurements. A Perkin-Elmer 521 grating infrared spectrophotometer, calibrated in the CO stretching region with CO and H_2O vapor, was used to obtain all frequency and rate data.

Calculations. All machine calculations were done on the IBM 7044 at the Tulane University Computing Center.

Results

Infrared Spectral Measurements. The infrared spectra of $NaMn(CO)_5$, $LiMn(CO)_5$, and the substituted derivatives $NaMn(CO)_4PR_3$ (where PR_3 = $P(OPh)_3$, PPh_3, and $PPhMe_2$) in the ν(CO) region are reported in Table I. Spectra of $NaMn(CO)_5$ are reported in Et_2O, THF, and in THF to which aliquots of HMPA (10 to 20 equiv of HMPA to Na^+ ion) and 15-crown-5 (1:1, 15-C-5:Na^+) have been added. Unfortunately the limited solubility of the phosphine and phosphite substituted derivatives in Et_2O prevented infrared studies in this solvent. The infrared spectra of $NaMn(CO)_5$ in THF and HMPA/THF solutions are shown in Figure 1. Spectrophotometric titration of $NaMn(CO)_5$ in THF with HMPA showed a gradual change of the five-band envelope in the 1950–1850-cm^{-1} region to a two-band envelope. The limiting spectrum was observed when 10 equiv of HMPA to Na^+ had been added. The THF spectrum has been analyzed as a mixture of anions experiencing a symmetrical solvent environment, i.e., solvent-separated ions (and/or free ions), and anions which experience a perturbation at one CO group. Brown and Pribula have proposed these latter contact ions to involve interaction of Na^+ ion with an axial CO ligand.[7] Comparison of the two spectra shown in Figure 1 by means of a quantitative band shape analysis indicates the mixture of species in THF to be composed of 48% contact ions and 52% solvent-separated (and/or free) ions at a total $NaMn(CO)_5$

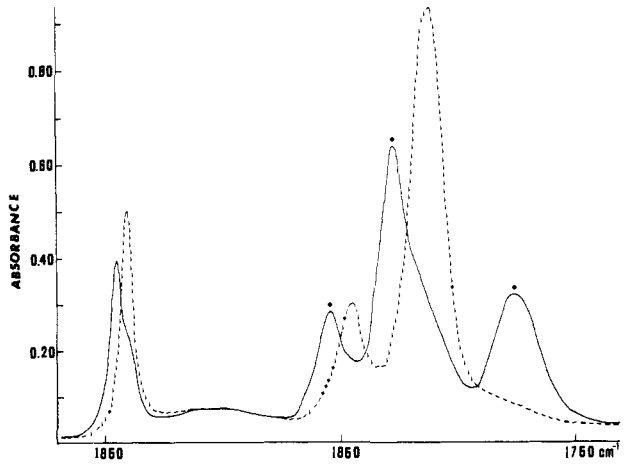

Figure 2. ν(CO) spectra of $NaMn(CO)_4PPh_3$ (* absorptions due to contact ion species): (—) 0.016 M in THF; (- - -) 0.016 M in THF with 6 equiv of HMPA to Na^+ added.

salt concentration of 6.7×10^{-3} M (see Figure 1 for the relative band areas).[13,14] As the total concentration of the sodium salt, $NaMn(CO)_5$, is decreased there is a concomitant decrease in the fraction which exists as contact ions; only 18% exists as contact ion pairs at a total salt concentration of 5.7×10^{-4} *M*. It is important to note here that although the two bands at 1893.7 and 1860.7 cm^{-1} in HMPA/THF correspond in frequencies and intensity ratio to two of the bands (1897.0 and 1862.3 cm^{-1}) in the THF spectrum, the identity of the species is not necessarily the same. That is, these two bands in THF undoubtedly correspond to the solvent-separated ion pairs whereas in HMPA/THF these correspond to other solvent-separated species and/or free ions. Unfortunately the effective symmetry and the effective field about the metal carbonyl anion is essentially identical for the two types of less associated species and infrared spectroscopy cannot distinguish between them. On the other hand, in diethyl ether solvent, $NaMn(CO)_5$ exists as approximately 100% contact ion pairs. At the other extreme the lithium salt, $LiMn(CO)_5$, exhibits the two-band ν(CO) spectrum in both THF and HMPA/THF which is ascribed to the solvent-separated or free ions. There is however a small amount of contact ion pairs present (<10%) in $LiMn(CO)_5$ in THF as shown by a slight change in band intensities upon addition of small quantities of HMPA.

Similarly the spectra of the phosphine and phosphite substituted derivatives exhibit a complex ν(CO) band pattern (at least six bands) in THF solution which is simplified to the expected three-band pattern for C_{3v} $Mn(CO)_4L^-$ derivatives upon addition of HMPA. The spectra in THF and HMPA/THF for the $[Ph_3PMn(CO)_4]Na$ derivative are depicted in Figure 2. In order to account for the number of ν(CO) absorptions (four) as well as their relative intensities[15] it is necessary to postulate Na^+ ion interaction at an equatorial carbonyl ligand rather than the axial carbonyl as was postulated by Pribula and Brown[7] for the unsubstituted derivative (see Figure 3). The fraction of ions which exists as contact ion pairs in THF solution in the phosphine and phosphite substituted derivatives, about 80–85%, is considerably greater than that observed in $NaMn(CO)_5$ in THF at similar concentrations. Although quantitative data were difficult to obtain, qualitatively there is no significant change in this distribution as the substituted ligand varies among Me_2PhP, Ph_3P, and $(PhO)_3P$ (there is possibly a slight increase in the solvent-separated ions for the less basic $(PhO)_3P$ derivative).

Cotton-Kraihanzel[16] CO force constant calculations for the solvent-separated or free ion C_{3v} $Mn(CO)_4L^-$ species were carried out employing the procedure we have recently described in detail for the isoelectronic $LFe(CO)_4$ analogues.[17]

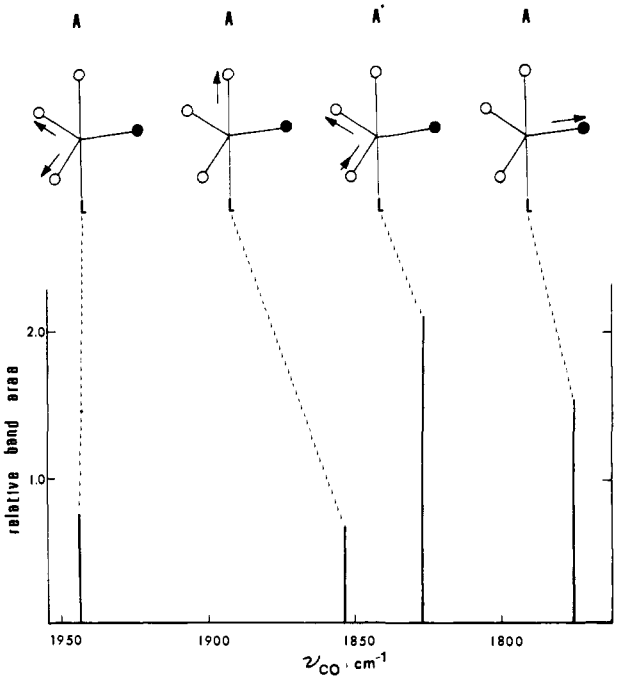

Figure 3. Vibrational assignment of ν(CO) absorptions in $NaMn(CO)_4L$ contact ion species. The relative band areas are those observed for the $NaMn(CO)_4PPh_3$ species (* absorptions in Figure 2).

Table II. Calculated Force Constants in Axially Substituted $LMn(CO)_4^-$ and $LFe(CO)_4$ Derivatives[a]

M	L	Force const, mdyn/Å[b]			
		k_1	k_2	$k_{c'}$	k_c
Mn	Me_2PhP	14.06	13.65	0.53_0	0.37_8
Fe	Me_2PhP	16.20	15.63	0.46_6	0.33_0
Mn	Ph_3P	14.13	13.78	0.51_0	0.36_4
Fe	Ph_3P	16.15	15.71	0.44_7	0.31_7
Mn	$(PhO)_3P$	14.47	14.14	0.50_1	0.35_8
Fe	$(PhO)_3P$	16.48	15.92	0.45_0	0.32_0

[a] Determined from frequency data obtained in HMPA/THF solution for $LMn(CO)_4^-$ and in hexane solution for $LFe(CO)_4$. [b] k_1, k_2, $k_{c'}$, and k_c refer to the axial, equatorial, equatorial-equatorial, and axial-equatorial constants, respectively. Calculations were done employing a $k_{c'}/k_c$ ratio of 1.40.[17]

These are listed in Table II and clearly indicate that the equatorial carbonyls' force constant, k_2, is significantly lower than the axial carbonyl force constant, k_1. A priori we would have predicted that Na^+ ion interaction would occur at the more negative equatorial oxygen atoms as inferred from the relative magnitudes of k_2 and k_1.[18,19] Force constants for the $LFe(CO)_4$ analogues are listed for comparison.

In addition, force constant calculations have been performed on the contact ion $Na^+Mn(CO)_4L^-$ species. In these cases the number of independent CO force constants far exceed the number of observed ν(CO) frequencies. Figure 4 describes the force constants employed in these calculations. It was therefore necessary to assume little change in the interaction constants from those in the solvent-separated or free ion $Mn(CO)_4L^-$ computations and to further make the approximations that $k_{c'} = k_{c''}$ and $k_c = k_{cc}$ (see Figure 4). Calculated values for the CO stretching force constants in the $Na^+Mn(CO)_4L^-$ contact ion pair species are listed in Table III.

Conductance. The equivalent conductances of all the alkali metal carbonylates studied vary with concentration in a manner similar to the sample data in Table IV. These data

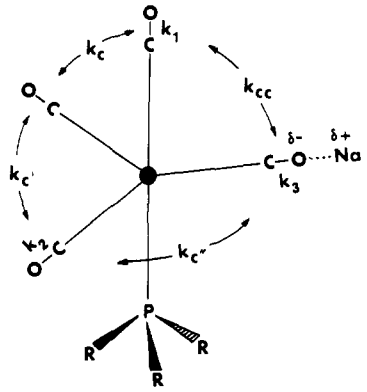

Figure 4. CO stretching force constants in $Na^+ \cdots OCMn(CO)_3PR_3^-$ derivatives. Approximations were that $k_c = k_{cc}$ and $k_{c'} = k_{c''}$.

Table III. Calculated Force Constants in Contact Ion Pairs of $NaMn(CO)_4L$ Derivatives[a]

L	Force const, mdyn/Å[b]				
	k_1	k_2	k_3	$k_{c'}$	k_c
Me_2PhP	14.31	13.84	12.94	0.51_3	0.41_1
Ph_3P	14.39	13.95	13.00	0.47_9	0.40_6
$(PhO)_3P$	14.56	14.34	13.43	0.54_2	0.35_9

[a] Determined from frequency data in THF. [b] k_3 corresponds to the CO ligand in contact with Na^+. For a description of the force field, see Figure 4.

were analyzed according to the Fuoss treatment of equilibria describing ion-pair to free ions (eq 3) and triple ion dissociation (eq 6):[20] associated ion pair–free ions equilibria, K_{diss}

$$CA \rightleftharpoons C^+ + A^- \quad (1)$$

or

$$CSA \rightleftharpoons CS^+ + A^- \quad (2)$$

$$F/\Lambda = 1/\Lambda_0 + c\Lambda f^2/K_{diss}\Lambda_0^2 F \quad (3)$$

triple ion equilibria, K_t

$$C_2A^+ \rightleftharpoons CA + C^+ \quad (4)$$

or

$$CA_2^- \rightleftharpoons CA + A^- \quad (5)$$

$$\Lambda c^{1/2} g(c) = \Lambda_0 K_{diss}^{1/2} + (\lambda_0 K_{diss}^{1/2}/K_t)(1 - \Lambda/\Lambda_0)c \quad (6)$$

The functions F, f, and $g(c)$ are respectively a function which corrects for thermal motion of the ions, the activity coefficient as expressed by $f^2 = \exp[-8.405 \times 10^6 c^{1/2}\Lambda^{1/2}F^{1/2}/D^{3/2}T^{3/2}\Lambda_0^{1/2}]$, and a function which corrects for the activity and mobility of triple ions. The dependence of the functions on Λ, Λ_0, concentration (c), viscosity (η), dielectric constant (D), and universal constants may be found in ref 20. A viscosity of 4.60×10^{-3} P and a dielectric constant of 7.39 for THF at 26.0 °C was taken from the work of Hogen-Esch and Smid.[21] The limiting conductance of the triple ion, λ_0, was approximated as ⅓ of Λ_0.[20] The conductivity of pure THF was beyond the lower limit of our bridge and assumed negligible in these studies. An initial graphical display of the data in terms of a plot of F/Λ vs. $c\Lambda f^2/F$ employed an approximation of Λ_0 based on literature studies in THF.[22] (Calculations were not very sensitive to the initial choice of Λ_0.) At lower concentrations the plots were linear and these data were subjected to a linear-least-squares fit which gave rise to a better estimate of Λ_0. The improved value of Λ_0 was then used to recalculate values of F and f. This process was iterated until the intercept converged. The final iterations are shown in Figure 5, and Λ_0 and K_{diss} values are given in Table V. An exact error may not be assigned to these data. The compounds are air sensitive; adventitious oxygen decreases conductance readings and its presence may be readily detected by observing continuous drifting as the readings are taken. Using extreme care to exclude air, reproducible data were obtained. The uncertainty in Λ_0 and K_{diss} for a similar system has been estimated as at least ±10%[22] and is most likely applicable here.

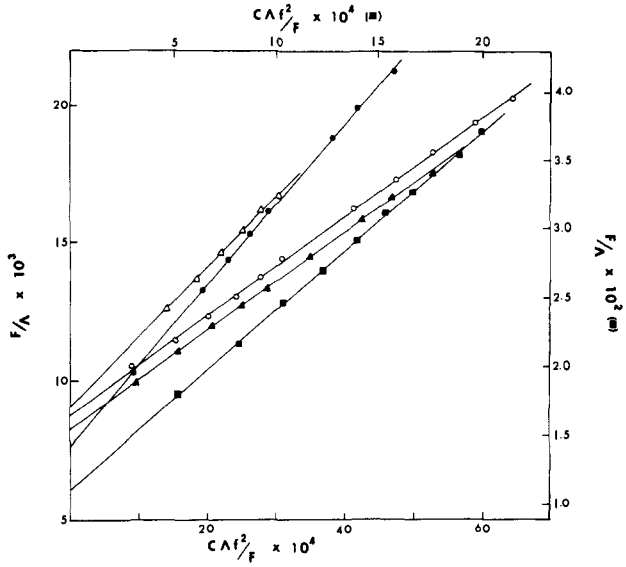

Figure 5. Fuoss plots in the $<10^{-4}$ M concentration region for: $NaMn(CO)_5$ (●); $LiMn(CO)_5$ (○); $[Na^+\cdot 15\text{-C-}5][Mn(CO)_5^-]$ (▲); $[Na^+\cdot HMPA][Mn(CO)_5^-]$ (△) (run in 5:1 HMPA:Na^+); and $NaMn(CO)_4P(OPh)_3$ (■) (scale to right and top of figure).

For all compounds studied, deviation from linearity in the initial F/Λ vs. $c\Lambda f^2/F$ plot appeared at ca. 1.3×10^{-4} M. The higher concentration region was analyzed according to eq 6. Linear plots of $\Lambda c^{1/2} g(c)$ vs. $(1 - \Lambda/\Lambda_0)c$ in this concentration region yielded the triple ion dissociation constants, K_t, also found in Table V. The K_{diss} values as obtained from the intercept were consistent with those obtained according to eq 3.

Center-to-center distances of ion pairs may be estimated from electrostatic sources (eq 7) or from hydrodynamic sources (eq 8),[23] where $\lambda_0^{\pm}$ is the limiting conductance contribution of each ion to the overall Λ_0 and η is the viscosity. The λ_0^+ for Na^+ and Li^+ in THF have been determined to be 48.2 and 36.6 $cm^2\ ohm^{-1}\ equiv^{-1}$, respectively.[24] Center-to-center distances as computed according to eq 7 and 8 are also listed in Table V. Limitations of these data due to assumptions inherent to the physical models used for eq 7 and 8 are discussed below. In the studies utilizing 15-crown-5 or HMPA-complexed Na^+, a λ_0^- of 80 $cm^2\ ohm^{-1}\ equiv^{-1}$, the average λ_0^- obtained from the $NaMn(CO)_5$ and $LiMn(CO)_5$ data, was assumed for $Mn(CO)_5^-$.

distance, d, electrostatic source

$$K_{diss} = (3000/4\pi N d^3)\exp(-e^2/dDkT) \quad (7)$$

Stokes radii, $r_{\pm}$, hydrodynamic source

$$10^8 r_{\pm} = 0.819/\lambda_0^{\pm}\eta \quad (8)$$

The equivalent conductances of $NaMn(CO)_5$ and $LiMn(CO)_5$ in THF increase as stoichiometric increments of HMPA or fractional stoichiometric increments of 15-crown-5 are added. Such conductometric titration curves are shown in Figure 6. With 15-C-5 as cation complexing agent a sharp change in slope is observed at a mole ratio near 1 for both Na^+ and Li^+. The predominant change in slope in the HMPA/Na^+

Table IV. Equivalent Conductances of Some Manganese Carbonylates in THF at 26 °C

$NaMn(CO)_5$		$[Na^+ \cdot 15\text{-C-}5][Mn(CO)_5^-]$[a]		$Na[Mn(CO)_4P(OPh)_3]$	
Concn, $\times 10^5$ M	Λ	Concn, $\times 10^5$ M	Λ	Concn, $\times 10^5$ M	Λ
1.23	93.8	1.23	97.2	1.16	54.0
3.67	71.6	2.46	86.3	2.32	44.4
4.90	65.8	3.67	79.0	3.47	38.9
6.12	61.6	4.90	73.9	4.62	35.2
7.34	58.1	6.12	70.1	5.77	32.4
12.20	49.1	8.55	63.8	6.92	30.4
14.60	46.1	9.11	66.1	8.06	28.6
18.20	43.0	12.20	57.7	9.21	27.4
30.0	36.2	14.60	54.5	10.30	26.3
58.60	29.0	18.20	51.2	11.50	25.1
85.90	25.4	30.0	44.0	13.80	23.4
112	23.4	41.60	40.0	17.10	21.7
160	21.0	58.60	35.9	28.30	17.7
205	19.5	85.90	32.0	55.20	13.8
284	17.8	112	29.5	80.9	12.0
351	17.0	160	26.7	105	10.9
		205	24.8	151	9.6
		246	23.7	193	8.86
		319	22.2	268	7.99
				331	7.54

[a] Prior to dilution, 1 equiv of 15-crown-5 (15-C-5) per Na^+ was added to the stock solution of $NaMn(CO)_5$.

Table V. Parameters Derived from Conductance Dependence on Concentration of $M^+Mn(CO)_4L^-$ in THF at 26.0 °C

Compd	$K_{diss} \times 10^5$[a]	Λ_0	d,[b] Å	r_+[c]	r_-[c]	$(r_+ + r_-)$	$K_t \times 10^3$
$NaMn(CO)_5$	1.98	131	6.9	3.70	2.15	5.9	6.38
$LiMn(CO)_5$	4.30	114	7.6	4.87	2.30	7.2	4.55
$[Na^+ \cdot 15\text{-C-}5][Mn(CO)_5^-]$	3.90	121	7.6	4.36	2.22[d]	6.6	5.34
$[Na^+ \cdot 5HMPA][Mn(CO)_5^-]$	3.16	111	7.4	5.76	2.22[d]	8.0	1.14
$NaMn(CO)_4P(OPh)_3$	0.93	91	6.3	3.70	4.16	7.9	6.60

[a] Obtained by analysis of data below 1.3×10^{-4} M according to eq 3; above this value, the data fit eq 6. [b] Ion center to center distance as computed according to Fuoss's eq 7. [c] Stokes radii (eq 8), computed assuming $\lambda_0^+(Li^+) = 36.6$ and $\lambda_0^+(Na^+) = 48.2$ in THF.[24] [d] $\lambda_0^-(Mn(CO)_5^-)$ assumed to be the average obtained from $NaMn(CO)_5$ and $LiMn(CO)_5$ data, 80 cm^2 ohm^{-1} $equiv^{-1}$.

Table VI. Rate Data for Reactions of $Mn(CO)_5^-$ and $Mn(CO)_4PR_3^-$ with Alkyl Halides at 25 °C

Salt[a]	RX	[RX]	Solvent[b]	$k_2 \times 10^3$, M^{-1} s^{-1} [c]
$NaMn(CO)_5$	$PhCH_2Cl$	0.086 04	Et_2O	69.0 ± 4
		0.414 0	THF	1.64 ± 0.03
		0.770 0	HMPA/THF	0.149 ± 0.003
		0.788 6	15-C-5/THF	0.40 ± 0.02
	$PhCH_2Br$	0.012 82	THF	294.0 ± 17
	Allyl Cl	0.583 4	THF	1.18 ± 0.01
	Allyl Br	0.016 0	THF	186.0 ± 39
$LiMn(CO)_5$	$PhCH_2Cl$	0.790 0	THF	0.96 ± 0.02
		0.790 0	HMPA/THF	0.101 ± 0.002
$NaMn(CO)_4P(OPh)_3$	$PhCH_2Cl$	0.212 0	THF	8.9 ± 0.20
		0.206 4	HMPA/THF	1.53 ± 0.02
$NaMn(CO)_4PPh_3$	$PhCH_2Cl$	0.212 0	THF	10.10 ± 0.02
		0.414 0	HMPA/THF	3.76 ± 0.13
$NaMn(CO)_4PMe_2Ph$	$PhCH_2Cl$	0.016 0	THF	131.0 ± 74
		0.016 0	HMPA/THF	103.0 ± 43

[a] Salt concentrations are 1.60×10^{-2} M except for the alkyl bromides where the salt concentration equals the listed concentration of the alkyl bromides. [b] Solvents of HMPA/THF contain 10:1 M excess of HMPA to salt; solvents of 15-C-5/THF contain 1:1 mol of 15-crown-5 to salt. [c] Error limits for the rate constant data are one standard deviation.

or $HMPA/Li^+$ titrations occurs at a mole ratio between 2 and 4. Further addition of HMPA continually increases Λ as the dielectric constant of the mixed solvent system increases.

Kinetic Measurements. The rate of nucleophilic addition reactions of $NaMn(CO)_5$, $LiMn(CO)_5$, and $NaMn(CO)_4PR_3$ (where $PR_3 = P(OPh)_3$, PPh_3, and PMe_2Ph) derivatives to the alkyl halides ($PhCH_2Cl$, $PhCH_2Br$, CH_2CHCH_2Cl, and CH_2CHCH_2Br) in ether solvents with and without cation complexing reagents is shown to obey the rate law (eq 9) which is first-order in each of the two reactants.

$$\text{rate} = k_2[NaMn(CO)_4L][R'X] \quad (9)$$

Values of the second-order rate constants, k_2, at 25 °C for reactions studied under a variety of conditions are given in Table VI. The reactions were all quantitative in product formation and for the reactions involving $NaMn(CO)_4PR_3$ with

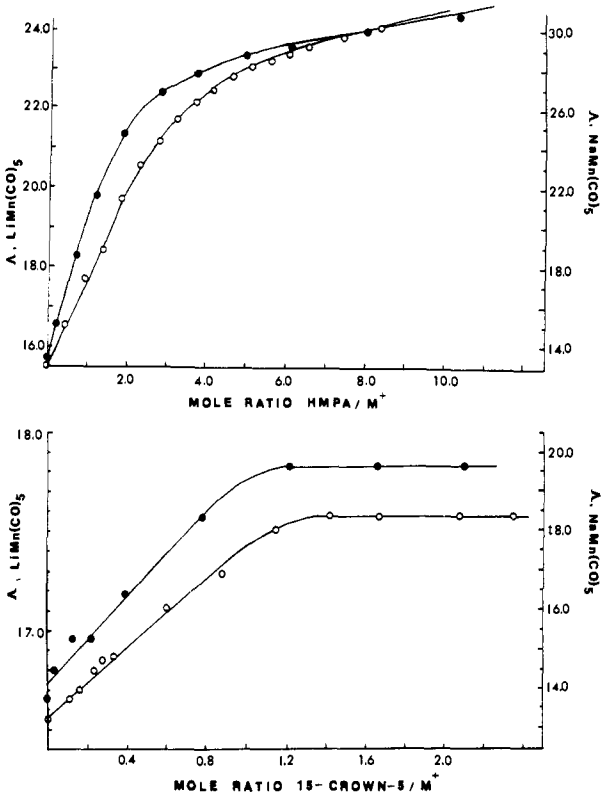

Figure 6. Conductometric titrations of 0.0123 M solutions of $NaMn(CO)_5$ (open circles) and $LiMn(CO)_5$ (closed circles) with HMPA and 15-crown-5.

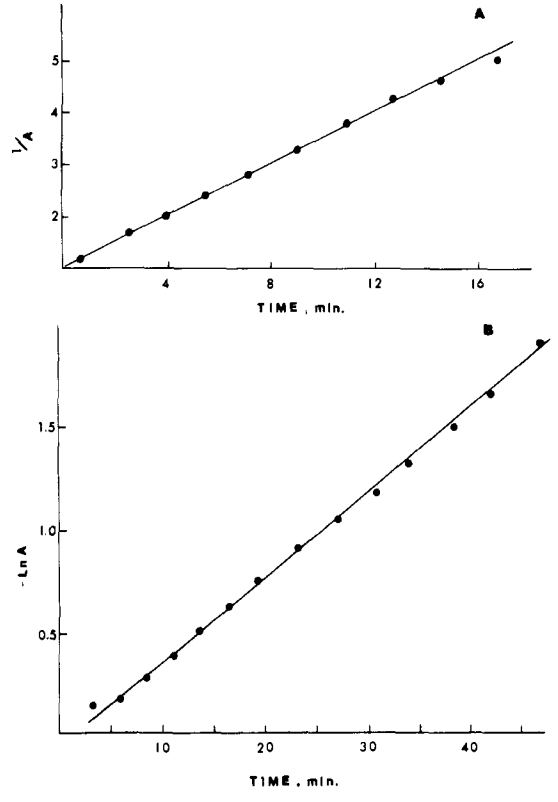

Figure 7. (A) Kinetic data for reaction of $NaMn(CO)_5$ and $PhCH_2Br$ run at $[NaMn(CO)_5] = [PhCH_2Br]$ in THF at 25 °C. (B) Kinetic plot utilizing pseudo-first-order conditions, $[PhCH_2Cl] \gg [NaMn(CO)_5]$, in THF at 25 °C.

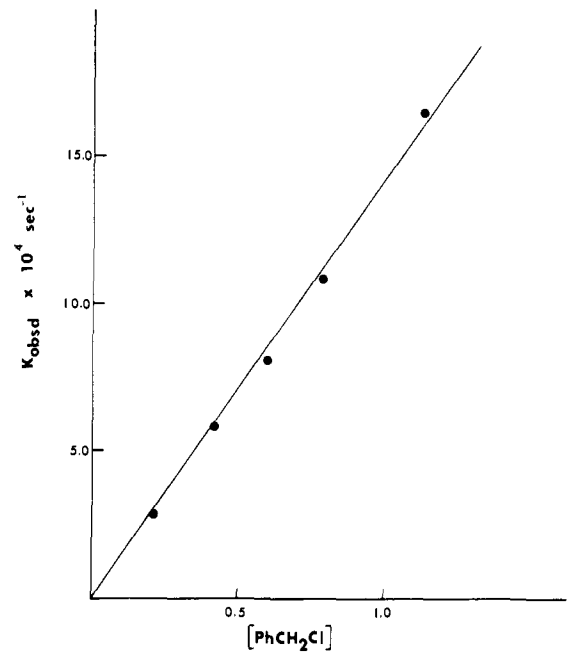

Figure 8. Demonstration of linear dependence of k_{obsd} on $[PhCH_2Cl]$ in the reaction of $NaMn(CO)_5$ and $PhCH_2Cl$ at 24.0 °C in THF.

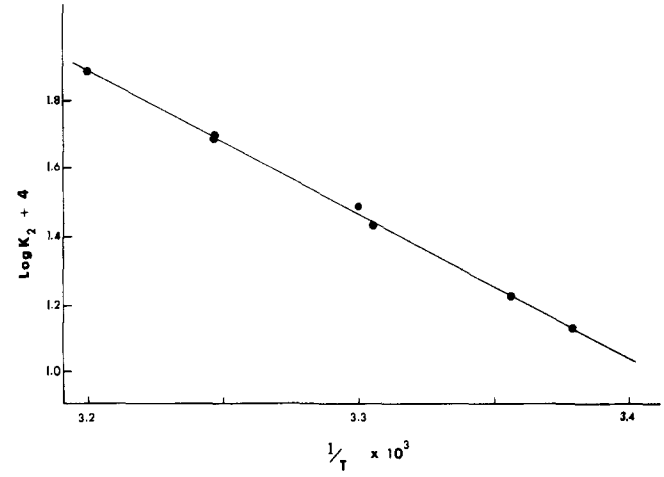

Figure 9. Representative Arrhenius plot shown here for reaction of $NaMn(CO)_5$ and $PhCH_2Cl$ in THF.

R'X the *cis*-$R'Mn(CO)_4PR_3$ isomers were exclusively produced. Linear pseudo-first-order and second-order (for reactions which were too rapid to be followed employing pseudo-first-order conditions) plots were obtained over the entire reaction as shown in Figures 7A and 7B for the disappearance of the manganese carbonyl anion species. Figure 8 demonstrates the first-order dependence on alkyl halide concentration for the reaction between $NaMn(CO)_5$ and $PhCH_2Cl$ in THF employing pseudo-first-order conditions. The observed rate constant was found to exhibit a linear dependence upon the $PhCH_2Cl$ concentration with a zero intercept over the range 0.212–1.133 M. This first-order dependence upon alkyl halide concentration was observed for all reactions investigated.

The second-order rate constants, k_2, were measured for several of the reactions investigated as a function of temperature and the activation parameters were determined. These data are given in Table VII and a representative Arrhenius plot is shown in Figure 9.

Figure 10 illustrates the effect on k_2 of addition of small quantities of HMPA to the reaction of $NaMn(CO)_5$ with $PhCH_2Cl$. The $\nu(CO)$ infrared spectra at these various $HMPA/Na^+$ ratios simultaneously show a decrease relative to that in pure THF in the amount of contact ion pairs with

Table VII. Activation Parameter Studies for Reactions of $NaMn(CO)_5$, $LiMn(CO)_5$, and $NaMn(CO)_4P(OPh)_3$ with Alkyl Halides

Salt	RX	Solvent	Temp, °C	$k_2 \times 10^3$, M^{-1} s^{-1} [c]	Activation parameters[d]
$NaMn(CO)_5$	$PhCH_2Cl$	THF	22.9	1.35 ± 0.05	
			25.0	1.64 ± 0.03	
			29.6	2.67 ± 0.02	ΔH = 20.2 ± 0.3 kcal mol^{-1}
			30.0	3.06 ± 0.05	
			35.0	4.89 ± 0.02	ΔS = −4.1 ± 1.0 eu
			35.0	4.90 ± 0.10	
			39.5	7.90 ± 0.10	
		HMPA[b]	25.0	0.149 ± 0.003	ΔH = 16.2 ± 0.7 kcal mol^{-1}
			30.0	0.221 ± 0.004	
			40.1	0.553 ± 0.002	ΔS = −21.7 ± 2.4 eu
			45.1	0.82 ± 0.030	
	$PhCH_2Br$[a]	THF	25.0	231 ± 13	ΔH = 13.0 ± 0.9 kcal mol^{-1}
			30.0	324 ± 71	
			35.0	471 ± 21	ΔS = −17.3 ± 3.3 eu
	Allyl Cl	THF	25.0	1.18 ± 0.09	ΔH = 18.1 ± 0.2 kcal mol^{-1}
			30.0	1.95 ± 0.02	
			35.0	3.18 ± 0.08	ΔS = −12.2 ± 0.6 eu
$LiMn(CO)_5$	$PhCH_2Cl$	THF	25.0	0.89 ± 0.02	
			25.0	0.96 ± 0.02	ΔH = 20.1 ± 0.9 kcal mol^{-1}
			30.0	1.56 ± 0.05	
			35.0	2.76 ± 0.06	ΔS = −4.9 ± 3.1 eu
			40.0	4.70 ± 0.10	
		HMPA[b]	25.0	0.101 ± 0.002	ΔH = 16.3 ± 0.7 kcal mol^{-1}
			35.0	0.255 ± 0.007	
			45.0	0.568 ± 0.009	ΔS = −2.2 ± 2.6 eu
$NaMn(CO)_4P(OPh)_3$	$PhCH_2Cl$	HMPA[b]	25.0	1.204 ± 0.006	ΔH = 14.7 ± 1.3 kcal mol^{-1}
			30.5	2.00 ± 0.09	
			35.0	2.62 ± 0.14	ΔS = −22.7 ± 4.3 eu
			40.0	4.04 ± 0.14	

[a] $PhCH_2Br$ = $NaMn(CO)_5$ = 1.282×10^{-2} M; all other reactions have a 20-fold excess or greater of alkyl halide. [b] These are THF solutions with HMPA added in 20-fold molar excess to salt. [c] Error limits for the rate constant data are one standard deviation. [d] Error limits represent 95% confidence limits.

increasing $HMPA/Na^+$ ratio. $HMPA/Na^+$ ratio vs. percent contact ion pair values are: (0) 48%, (1) 30%, (2) 20%, and (4) 8%. The rate constant, k_2, is observed to decrease as the $HMPA/Na^+$ ratio increases; at a ratio of 3 to 5 equiv of HMPA to Na^+ the limiting value of k_2 is essentially achieved.

Discussion

All of the salts studied by conductivity techniques (10^{-4}–10^{-6} M) behaved according to an equilibrium of associated ion pairs with free ions. Above ca. 1×10^{-4} M the conductivity data of the salts followed triple ion behavior with K_t's on the order of 10^{-3}. (The value of 10^{-4} M is in good agreement with Fuoss's theoretical prediction of the critical concentration (1.3×10^{-4} M) for the formation of triple ions in a solvent such as THF.[20]) Thus at the concentrations of the infrared and kinetic studies (ca. 0.01 M), species I, IIIa, and IV of the following

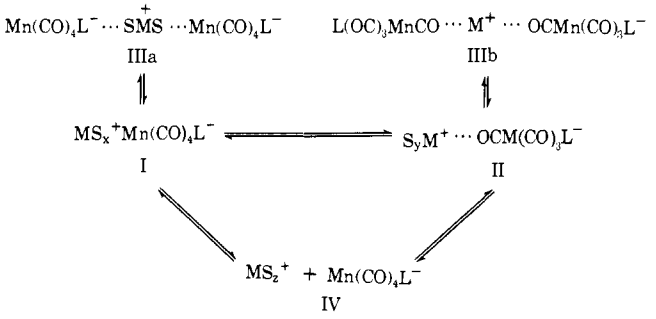

equilibria are expected to predominate for $LiMn(CO)_5$, $[Na^+ \cdot 15\text{-C-}5][Mn(CO)_5^-]$, and $[Na^+ \cdot x\text{HMPA}][Mn(CO)_5^-]$, and a mixture of all five species, for $NaMn(CO)_5$ and $NaMn(CO)_4L$. The precise description of the molecular arrangement is based both on the infrared analysis and on the conductance data, and a discussion of those arguments follows.

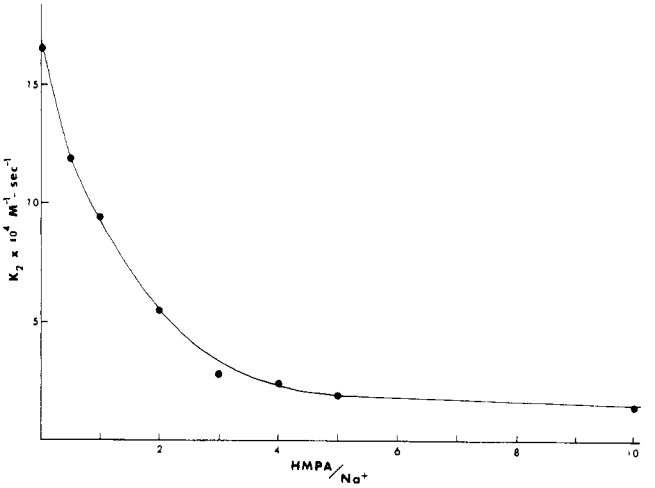

Figure 10. Dependence of second-order rate constant on mole ratio of HMPA to Na^+ for reaction of $NaMn(CO)_5$ and $PhCH_2Cl$ in THF at 25.0 °C.

Infrared spectra (10^{-2}–10^{-3} M) give a direct indication of the carbonyl anion environment. The manganese carbonylate is in a symmetrical environment for $LiMn(CO)_5$ in THF; an asymmetrical environment leads to more complex spectra for the sodium salts of $Mn(CO)_5^-$ and $Mn(CO)_4L^-$. The increased stability of a $Li^+ \cdot n$THF solvate over $Na^+ \cdot n$THF is generally expected and argues well for the observation here.

Interaction of a cation with the manganese carbonylate is expected to occur at the most electron-rich carbonyl oxygen atom assuming there are no steric restrictions. The lower value of the CO stretching force constant for the equatorial CO groups (k_2 in Table II) as compared with that of the axial CO

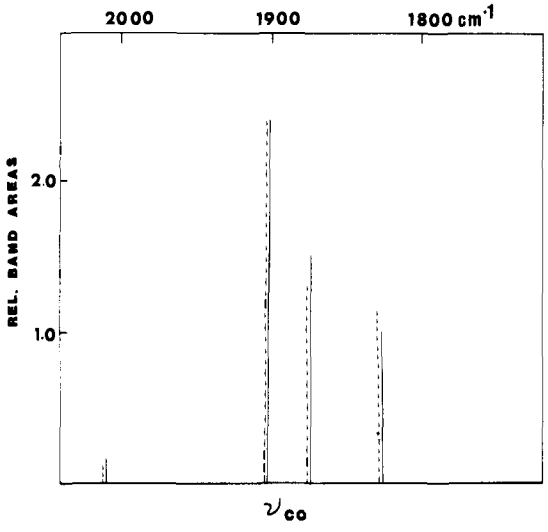

Figure 11. Calculated (—) and observed (- - -) intensity pattern for the ν(CO) absorptions of the contact ion species of $NaMn(CO)_5$ in THF.

group(s) (k_1 in Table II) indicates the equatorial carbonyl oxygen atoms are more electron rich in these $Mn(CO)_4L^-$ anions (L = phosphorus ligand or CO).[18,19,25,26] Contact ion interaction results in an increase in the complexed CO group's π acceptor ability. It has been demonstrated that stronger π-bonding ligands prefer to occupy the equatorial position in a trigonal bipyramidal structure.[27] Hence cation interaction at an equatorial CO ligand is further anticipated, and indeed the best fit of ν(CO) spectra with ir expectations and intensities was obtained for the $Mn(CO)_4L^-$ salts in THF assuming equatorial CO perturbation. A reexamination of the $NaMn(CO)_5$ spectrum in THF led us to conclude that the cation interaction is with the equatorial CO oxygen in that contact ion species as well. The assignments, alternative to those of Brown and Pribula,[7] are as follows: the weak vibration at 2009.0 cm^{-1} is A_1 under C_{2v} local symmetry; the most intense absorption at 1901.7 is the accidentally degenerate $A_1 + B_1$; the 1875.1 is the B_2; and the 1828.6 band is assigned to the CO complexed to Na^+, A_1.[28] This assignment is particularly attractive in light of the fact that the calculated intensity pattern (assuming all the dipole moment derivatives are essentially equivalent) agrees very well with that observed (see Figure 11).[29]

The change in the CO stretching force constant upon complexation (k_2 for the solvent-separated or free ion minus k_3) should reflect the extent of MCO···Na^+ interaction. For the phosphine and phosphite substituted derivatives ($k_2 - k_3$) ranges from 0.78 to 0.71, whereas for $NaMn(CO)_5$ ($k_2 - k_3$) is 0.65. These changes are in agreement with the observation that contact ion formation is more extensive in the phosphine substituted species.

It is important to note that the formal analysis given for a single carbonylate interacting with a cation also holds for a triple ion such as species IIIb. For example, the carbonyl stretching spectrum of $[\eta^5\text{-}C_5H_5Mo(CO)_3]_2Mg(py)_4$ both as a nujol mull and in pyridine solution is that expected for the tricarbonyl anion containing one perturbed CO group; i.e., no observable coupling occurs between the two carbonylates linked by the $Mg(py)_4^{2+}$.[5]

Further or corroborative information as to the molecular structure of the ionic species in solution may be obtained from parameters derived from conductance data. Center-to-center distance entries in Table V as derived according to eq 7 are particularly suspect in the cases of $NaMn(CO)_5$ and $NaMn(CO)_4P(OPh)_3$ where extensive contact ion interaction occurs. The sphere in continuum model which leads to eq 7 is not applicable to small cations which interact strongly with both solvent and anion.[30] Since the specific solvent shell of Li^+ effectively increases the size of this cation to that which would be expected to have a nonspecific interaction with the bulk solvent, the value of 7.6 Å is expected to accurately reflect the center-to-center ionic distance. Indeed if one assumes a linear arrangement such as the following, in which Mn-C is taken

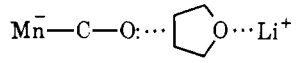

as 1.8 Å,[26] C-O as 1.1 Å,[26] the covalent radius of O as 0.7 Å, and the THF···Li^+ contribution of 4.2 Å (from molecular models and ref 21), the distance predicted is on the order of 7.8 Å. (The assumption of a linear arrangement is to provide a maximum estimate.) Center-to-center distances, d, for $NaMn(CO)_5$ and $NaMn(CO)_4P(OPh)_3$ are considerably smaller and, as stated before, purportedly inherently incorrect due to the inaccuracy of the macroscopic dielectric constant in the vicinity of the contact ion pair (species II). However, the values obtained, 6.3 Å for $NaMn(CO)_4P(OPh)_3$ and 6.9 Å for $NaMn(CO)_5$, are in the expected order for increased interaction and/or increased numbers of the contact ion pairs over the solvent-separated ion pairs for the former derivative. These data would also suggest that center-to-center distances in the asymmetric anion reflect specific points of attachment, i.e., in this case in the vicinity of the CO groups, rather than a distance based on the center of gravity of this much larger anion.

The second type of distance entries in Table V are based on λ_0^- and λ_0^+ estimates, eq 8. The Stokes radii computations reflect the size of an ion as based on its solution mobility at concentrations approaching zero; thus in the case of highly solvated ions, the average radius will include the ion plus its solvent shell. For large anions in a solution of low dielectric constant, little solvation is expected. Previously determined λ_0^+ values for Na^+ and Li^+ in THF were used in conjunction with our Λ_0 values to determine λ_0^- and hence r_- for $Mn(CO)_5^-$. The values obtained are very close, 2.15 and 2.30 Å, but they are considerably smaller than the 3.6 Å predicted from the estimated center of manganese to exterior of oxygen in a single Mn-C-O linkage. The Stokes radius, however, is that of a sphere which hydrodynamically behaves as does the corresponding ion and is derived according to a charged sphere model. An estimate of r_- for $Mn(CO)_5^-$ based on bond distance data would describe a sphere containing considerable free volume. In addition, the usual limitation of Stokes radii computations applies.[3] Whereas these data may not be compared directly with crystal structure data, the set may be examined for consistency within itself.

The r_- value of 4.16 Å obtained for $Mn(CO)_4P(OPh)_3^-$ is reasonably compared to that of $Mn(CO)_5^-$ in that molecular models would suggest this anion to have approximately twice the bulk of the unsubstituted carbonylate. This compound affords the most striking difference between the two distance estimates, d, as estimated from the K_{diss} parameter, and ($r_+ + r_-$) as estimated from limiting conductance data. The former parameter reflects some contact ion pairing at a specific site on the anion, and the latter reflects the actual bulk of the ions free in solution.

The consistency of the two determinations of λ_0^- (and r_-) for $Mn(CO)_5^-$ prompted an evaluation of λ_0^+ and r_+ of the two complexed salts, $[Na^+\cdot 15\text{-}C\text{-}5][Mn(CO)_5^-]$ and $[Na^+\cdot x\text{HMPA}][Mn(CO)_5^-]$. The lower limiting conductance of the 15-crown-5 and HMPA complexed Na^+ salts as compared to that in the pure THF solution is in agreement with a specific solvation of the Na^+ by these bulky complexing agents and an effective decreased mobility of the sodium in its new solvent shell. Assuming a λ_0^- for the $Mn(CO)_5^-$ to be the average obtained from the $NaMn(CO)_5$ and $LiMn(CO)_5$ data, r_+ for

$[Na^+ \cdot 15\text{-C-}5 \cdot n\text{THF}]$ and for $[Na^+ \cdot x\text{HMPA} \cdot y\text{THF}]$ are determined to be 4.36 and 5.76 Å, respectively. It should be emphasized that n, x, and y in the above expressions are averaged values. A coordination of two or more molecules of HMPA to one Na^+ (in accordance with the conductometric titrations) would certainly account for a larger average radius for the phosphoramide-complexed cation as compared to $Na^+ \cdot 4\text{THF}$.[31]

The concentration conductance dependence above suggests that cation-complexing agents such as HMPA and 15-crown-5 do not completely "free" the ion pairs, but rather promote the solvent-separated species and concomitantly a slight increase of K_{diss} over the pure THF solution of $NaMn(CO)_5$. Conductometric titrations (Figure 6) indicate a specific interaction of 2 to 4 molecules of HMPA to Na^+ or to Li^+ in $M^+Mn(CO)_5^-$, and of 1 molecule of 15-crown-5 to each Na^+ or Li^+ at salt concentrations of 0.012 M. Based on Pederson's original observations on the macrocyclic crown ethers, complexation of the smaller Li^+ cation with 15-C-5 is expected to be less favorable than complexation of Na^+, whose ionic diameter more nearly approximates the hole size of 15-C-5, and whose solvent shell should be less tightly held.[32] The available thermodynamic data generally agree with this expectation;[33] however, complexation of a cation whose ion diameter is smaller than the crown ether cavity size does occur and is to be noted here. The breaks in the titration curves (Figure 6) are especially dramatic in the case of the cyclic polyether for both Na^+ and Li^+. However, the total equivalent conductance changes very little in going to the 15-C-5 complexed salt, approximately 1 unit for the Li^+ salt and 5 units for the Na^+ salt. A somewhat larger change in Λ is observed upon addition of HMPA to the salt solutions.

Other evidence for the specific complexation of the Na^+ and Li^+ carbonylates with 15-C-5 and HMPA comes from the kinetic studies. A dramatic lowering of reaction rate in the presence of cation complexing agents is shown in Figure 10 and in Table VI. Clearly superimposed on the solvent or cation effect is also the rate-determining electronic effect of substituent L, i.e., k_2 decreases for $PhCH_2Cl$ addition to $NaMn(CO)_4L$ in the order $PMe_2Ph > PPh_3 > P(OPh)_3 > CO$. The magnitude of the cation complexation rate depression is in the reverse order. The dependence of rate on alkyl halide is identical with that found for solvolysis of the halides, $PhCH_2Br > CH_2CHCH_2Br > PhCH_2Cl > CH_2CHCH_2Cl$.[34]

It is however the activation energy parameters that are most significant in discerning the rate dependence on reaction site structure. The data in Table VII indicate the impediment to reaction rate in the presence of a cation complexing agent such as HMPA lies in the entropy of activation. Indeed the enthalpy of activation is slightly reduced in solutions containing HMPA. One would conclude that the order or bulk of the transition state is substantially increased in such solutions.[34,35] The significance of this is that the solvated cation is still in the primary solvent shell of the anion. Various interpretations of the import of this toward mechanistic detail may be forwarded. For example, assuming the necessity of an expanded coordination number for manganese in the transition state, the larger negative entropy in the HMPA solvates may be due to rearrangements involving the carbonylate still aggregated to the much bulkier $Na^+ \cdot x\text{HMPA} \cdot y\text{THF}$ or $Li^+ \cdot r\text{HMPA} \cdot s\text{THF}$. That is, the number of configurations to be assumed by the transition state is reduced in the presence of the bulky, tightly solvating, HMPA. Alternatively a second hypothesis involves an R′X displacement of solvent molecule, presumably a less tightly held THF, in the solvation sphere of the cation, and sodium ion assistance in polarizing the R′X bond is envisaged. The large negative entropy in the HMPA solvate would be ascribed to the necessity of rearrangement of the bulky HMPA's on the solvation sphere of the Na^+ as compared to the smaller THF molecules. The importance of sodium ion assistance in R′X bond cleavage gains support on examination of the entropy data for various R′X (Table VII). There is a significant decrease in entropy in the reaction of $NaMn(CO)_5$ in THF as the polarizability of the R′X bond increases in the series $PhCH_2Cl$ (−4.1 eu) < CH_2CHCH_2Cl (−12.2 eu) < $PhCH_2Br$ (−17.3 eu). Simultaneously the enthalpy has decreased, in accordance with an inherently weaker R′X bond in addition to the proposed sodium-facilitated bond breakage.

Obviously a combination of the two proposals discussed above, expansion of the coordination number of Mn and sodium ion assistance in R′X bond breakage, may be operative in these reactions.

Acknowledgment. The authors express appreciation to Mr. H. H. Nelson, III, for assistance in the computations and to Professor H. P. Hopkins, Jr. (Georgia State University), for valuable discussion. The authors are grateful to the donors of the Petroleum Research Fund, administered by the American Chemical Society, which supported this research. In addition, we acknowledge the Research Corporation for a Cottrell Research Grant to D.J.D. and M.Y.D. for the purchase of the Perkin-Elmer 521 infrared spectrophotometer.

References and Notes

(1) Petroleum Research Fund Postdoctoral Fellow, 1973–1975.
(2) "Ions and Ion Pairs in Organic Reactions", Vol. I, M. Szwarc, Ed., Wiley-Interscience, New York, N.Y., 1972.
(3) M. Szwarc, "Carbanion Living Polymers and Electron Transfer Processes", Wiley, New York, N.Y., 1968.
(4) "Solute-Solvent Interactions", J. F. Coetzee and C. D. Ritchie, Ed., Marcel Dekker, New York, N.Y., 1969.
(5) S. W. Ulmer, P. M. Skarstad, J. M. Burlitch, and R. E. Hughes, *J. Am. Chem. Soc.*, **95**, 4469 (1973).
(6) For a review of Edgell's work in this area, see ref 2, Chapter 4, and references therein, especially W. F. Edgell, M. T. Yang, and N. Koizumi, *J. Am. Chem. Soc.*, **87**, 2563 (1965); W. F. Edgell and J. Lyford, IV, *ibid.*, **93**, 6407 (1971).
(7) C. D. Pribula and T. L. Brown, *J. Organomet. Chem.*, 71, 415 (1974).
(8) J. P. Collman, J. N. Cawse, and J. I. Braumann, *J. Am. Chem. Soc.*, **94**, 5905 (1972).
(9) M. Y. Darensbourg and D. Burns, *Inorg. Chem.*, **13**, 2970 (1974).
(10) D. Drew, D. J. Darensbourg, and M. Y. Darensbourg, *Inorg. Chem.*, **14**, 1579 (1975).
(11) D. Drew, M. Y. Darensbourg, and D. J. Darensbourg, *J. Organomet. Chem.*, **85**, 73 (1975).
(12) G. Jones and B. C. Bradshaw, *J. Am. Chem. Soc.*, **55**, 1780 (1933).
(13) Band shape analysis was carried out employing our previously published procedure.[14] Because of the gross overlapping of the two high-frequency bands (one each belonging to the contact ion and solvent-separated ion, respectively) in the five-band envelope of $NaMn(CO)_5$ in THF it was necessary to resolve these two components as one absorption. Since the ratio of the two bands due to the solvent-separated or free ion was independently determined in HMPA/THF solution and the low-frequency component of the solvent-separated species in the THF spectrum was resolvable, it was therefore possible to divide the intensity of the composite high-frequency band into its components as shown in Figure 1.
(14) C. L. Hyde and D. J. Darensbourg, *Inorg. Chem.*, **12**, 1075 (1973).
(15) The intensities of the four CO vibrational modes are related to the dipole moment change during the CO stretch (μ'_{MCO}) and α (half the angle between the two uncomplexed equatorial CO groups) assuming no coupling of the three A vibrations in the following manner: $I_A = 2G_{tt}\cos^2\alpha(\mu'_{MCO})^2$, $I_{A'} = G_{tt}(\mu'_{MCO})^2$, I_A(complexed) = $G_{tt}(\mu'_{MCO})^2$, and $I_{A''} = 2G_{tt}\sin^2\alpha(\mu'_{MCO})^2$. Therefore, assuming all the μ'_{MCO}'s are approximately equivalent and $\alpha = 60°$, $I_A:I_{A'}:I_A$(complexed):$I_{A''} = 0.50:1.0:1.0:1.5$ or $(I_A + I_A + I_A):I_{A'} = 1.67:1$. The observed ratio is 1.43. On the other hand for an axial $Na^+\cdots$OC–M$^-$ interaction three infrared absorptions would be expected; $A_1 + A_1$(complexed) + E. The expected intensity ratio would be $(I_{A_1} + I_{A_1}):E = 1:3$ or 0.33.
(16) F. A. Cotton and C. S. Kraihanzel, *J. Am. Chem. Soc.*, **8**, 4432 (1962).
(17) D. J. Darensbourg, H. H. Nelson, III, and C. L. Hyde, *Inorg. Chem.*, **13**, 2135 (1974).
(18) D. J. Darensbourg and M. Y. Darensbourg, *Inorg. Chem.*, **9**, 1691 (1970).
(19) M. Y. Darensbourg, H. L. Conder, D. J. Darensbourg, and C. Hasday, *J. Am. Chem. Soc.*, **95**, 5919 (1973).
(20) R. M. Fuoss and F. Accascina, "Electrolytic Conductance", Interscience, New York, N.Y., 1959.
(21) T. E. Hogen-Esch and J. Smid, *J. Am. Chem. Soc.*, **88**, 318 (1966).
(22) E. C. Ashby, F. R. Dobbs, and H. P. Hopkins, Jr., *J. Am. Chem. Soc.*, **95**, 2823 (1973).
(23) See ref 3, Chapter V, for a discussion of center to center distance computations and assumptions.
(24) D. N. Bhattacharya, C. L. Lee, J. Smid, and M. Szwarc, *J. Phys. Chem.*, **69**, 608 (1965).
(25) Force constants for $Mn(CO)_5^-$ are found in ref 7 (k_1 = 15.05 and k_2 =

14.36). Support for this also comes from the x-ray structural analysis of $Mn(CO)_5^-$ where the equatorial Mn–C bond lengths are slightly shorter (0.02 Å) than the corresponding axial bond lengths.[26]
(26) B. A. Frenz and J. A. Ibers, *Inorg. Chem.*, 11, 1109 (1972).
(27) A. R. Rossi and R. Hoffmann, *Inorg. Chem.*, **14**, 365 (1975).
(28) The force field computed which fits this assignment is $k_1 = 15.20$, $k_2 = 14.55$, $k_3 = 13.71$, $k_{c'} = k_{c''} = 0.35_3$, $k_c = k_{cc} = 0.32_6$, and $k_t = 0.59_4$.
(29) This is contrary to the assignment involving an axial interaction where the intensity pattern observed is in very poor agreement with that computed. This is particularly noticeable when one examines the diethyl ether spectrum which is predominantly the contact ion species.
(30) A. D'Aprano and R. M. Fuoss, *J. Phys. Chem.*, **67**, 1722 (1963); T. L. Fabry and R. M. Fuoss, *ibid.*, **68**, 907 (1964).
(31) E. C. Ashby, F. R. Dobbs, and H. P. Hopkins, Jr., *J. Am. Chem. Soc.*, **97**, 3158 (1975).
(32) C. J. Pedersen, *J. Am. Chem. Soc.*, **89**, 7017 (1967); *ibid.*, **92**, 386 (1970); *ibid.*, **92**, 391 (1970).
(33) J. J. Christensen, D. J. Eatough, and R. M. Izatt, *Chem. Rev.*, **74**, 351 (1974); H. K. Frensdorff, *J. Am. Chem. Soc.*, **93**, 600 (1971).
(34) "Solvolytic Displacement Reactions", A. Streitwieser, Jr., McGraw-Hill, New York, N.Y., 1962.
(35) N. Ivanoff and M. Magat, *J. Chim. Phys. Phys.-Chim. Biol.*, **47**, 914 (1950); E. Bauer and M. Magat, *ibid.*, **47**, 922 (1950).

Photochemistry of Organic Ions in the Gas Phase. Comparison of the Gas Phase Photodissociation and Solution Absorption Spectra of Benzoyl Cation, Protonated Benzene, and Protonated Mesitylene

B. S. Freiser and J. L. Beauchamp*[1]

Contribution No. 5148 from the Arthur Amos Noyes Laboratory of Chemical Physics, California Institute of Technology, Pasadena, California 91125. *Received July 31, 1975*

Abstract: The gas phase photodissociation spectra of benzoyl cation, protonated benzene, and protonated mesitylene are reported and compared to their solution absorption spectra. Each ion exhibits two maxima in the wavelength region 2000–4000 Å. The values of λ_{max} for the benzoyl cation ($C_6H_5CO^+ + h\nu \rightarrow C_6H_5^+ + CO$) are 260 ± 10 nm ($\sigma \simeq 0.15$ Å^2) and 310 ± 10 nm ($\sigma \simeq 0.04$ Å^2), for protonated benzene ($C_6H_7^+ + h\nu \rightarrow C_6H_5^+ + H_2$) 245 ± 10 nm ($\sigma \simeq 0.02$ Å) and 330 ± 10 nm ($\sigma \simeq 0.08$ Å^2), and for protonated mesitylene ($C_9H_{13}^+ + h\nu \rightarrow$ products) 250 ± 10 nm ($\sigma \simeq 0.06$ Å^2) and 355 ± 10 nm ($\sigma \simeq 0.10$ Å^2). With the exception of protonated benzene, excellent agreement between the solution absorption spectra and gas phase photodissociation spectra is observed. The lack of agreement for protonated benzene is attributed to other absorbing species present in solution. From a comparison of the gas phase and solution spectra, it can be inferred that the quantum yields for photodissociation do not vary significantly with wavelength and are thus very likely close to unity. In addition, there is no detectable solvent shift for any of the observed transitions.

Solvent shift is an effective spectroscopic tool both for determining the character of absorption bands in organic molecules and for yielding insight into the intermolecular forces between solute and solvent.[2] In general solvent shifts serve as a sensitive probe of the change in charge distribution which accompanies electronic excitation. It is possible, for example, to distinguish $n \rightarrow \pi^*$ transitions from $\pi \rightarrow \pi^*$ transitions in azo compounds, aldehydes, ketones, and thioketones by using solvents having a range of dielectric constants.[3] The highly specific solvent shifts observed in the presence of hydroxylic solvents are useful to identify transitions involving an n-donor site and can be interpreted to yield hydrogen bond strengths.[4] In the extreme cases where the solvent effects a change in the chemical species present, solvent shift enables the study of acid–base equilibria, tautomeric equilibria, and complex formation.[5]

Numerous examples of electronic absorption spectra of carbocations in solution are available in the literature.[6] These experiments are usually performed in superacid media having extremely low nucleophilicity where the ions are stable. In many instances it has been observed that the ions are so strongly solvated that the spectra are independent of the counterion present.[7]

Gas phase absorption spectra provide the standard by which absolute solvent shifts of carbocations can be determined. However, obtaining these spectra directly is rendered virtually impossible by the difficulties associated with producing and maintaining the required ion densities.[8] Ion cyclotron resonance spectroscopy (ICR)[9] provides the desired spectroscopic information from photodissociation spectra obtained by determining the wavelength dependence of processes such as generalized in eq 1.[10-12] Absorption maxima determined by

$$A^+ + h\nu \rightarrow B^+ + C \qquad (1)$$

this method should yield an intrinsic measure of the vertical transition energies of the ion since the photodissociation spectrum is free of all effects due to solvent, counterions, and any other neutral or ionic species which absorb in the region of interest. A meaningful comparison to the theoretical transition energies in addition to solvent shift data may therefore be obtained. Band intensities in photodissociation spectra depend, however, not only on the intrinsic transition probability or gas phase extinction coefficient, $\epsilon_g(\lambda)$, but also on the photodissociation quantum yield, $\varphi_d(\lambda)$. The measured quantity is the photodissociation cross section, $\sigma_d(\lambda)$, which is proportional to the product of these variables (eq. 2). If the quantum

$$\sigma_d(\lambda) \propto \epsilon_g(\lambda)\varphi_d(\lambda) \qquad (2)$$

yield for photodissociation is relatively constant over an absorption band (Figure 1, band I), then $\sigma_d(\lambda)$ will reflect the absorption spectrum and directly yield the vertical excitation energy. If, on the other hand, φ_d varies significantly over an absorption band (Figure 1, band II), then $\sigma_d(\lambda)$ will not yield exactly the vertical excitation energy. The latter would occur, for example, in the vicinity of the thermodynamic threshold for dissociation, below which $\varphi_d(\lambda) = 0$.

To explore these ideas and investigate solvent effects on excitation energies of carbocations we have undertaken a study of the photodissociation spectra of species for which solution spectra are already available. We wish to report results for